NUMERICAL STUDY OF SEPARATED BOUNDARY LAYER TRANSITION UNDER PRESSURE GRADIENT

HuaJun Li

Department of Engineering and Design,
University of Sussex,
Brighton, BN1 9RH
United Kingdom,
E-mail: hl250@sussex.ac.uk

Zhiyin Yang

Department of Engineering,
College of Engineering and Technology
University of Derby,
Derby, DE22 3AW
United Kingdom,
E-mail: Z.Yang@derby.ac.uk

ABSTRACT

Large-eddy simulation (LES) is conducted to study the transition process of a separated boundary layer on a flat plate with an elliptical leading edge. A streamwise pressure distribution is imposed and the free stream turbulence intensity is 3% to mimic the suction surface of a low-pressure turbine (LPT) blade. A dynamic sub-grid scale model is employed in the study and the current LES results compare well with available experimental data and previous LES results. The transition process has been analysed with a particular focus on primary instabilities at work. Streaky structures further upstream of the separation, known as the Klebanoff Streaks, have been observed. Typical two-dimensional Kelvin-Helmholtz (K-H) rolls are distorted in the separated region. When Klebanoff streaks passing over a full-span K-H roll, portion of the two-dimensional roll merges with the Klebanoff streaks and develop into chaotic three-dimensional structures, whereas the remaining undisrupted two-dimensional K-H rolls develop into Λ-vortex indicating that despite the disturbances before separation, the K-H instability may still be the main instability at work.

INTRODUCTION

Transition process in attached boundary layer under low free stream turbulence level usual starts with the viscous Tollmien-Schlichting (T-S) instability or so called the T-S waves. Whereas for separated boundary layer it is well established that transition occurs due to the inviscid Kelvin-Helmholtz (K-H) instability. On a typical LPT blade suction surface in modern aero engines, the initially developed attached laminar boundary layer may separate due to an adverse pressure gradient (APG). Transition process in such a case becomes even more complex as both the T-S and K-H instabilities are possibly at work and may interact with each other too.

The transition process via the T-S instability in attached boundary layer has been well established under low free stream turbulence level and it is also evident that the main instability at work for separated boundary layer transition is the K-H mechanism. However there have been few studies on transition process involving both the T-S and the H-K instabilities. In recent studies of transition is separation bubbles with low background disturbances, Roberts and Yaras [1] detected the T-S wave in the attached boundary layer portion before separation, whereas McAuliffe and Yaras [2] detected the T-S wave in both attached and detached shear layer. Hughes and Walker [3] showed that the T-S wave has significant impact in their compressor blade design study.

The above cited studies were carried out at relatively low free stream turbulence level and the current study is focusing on the instability mechanisms at higher free stream turbulence level, identifying if both the T-S and the K-H instabilities are still at work, which one is more influencing and their interactions with each other.

NOMENCLATURE

So	[mm]	*Test section length*
U_{in}	[m/s]	*Uniform inflow velocity*
U_{out}	[m/s]	*Mean free stream velocity at x/So = 1*
U_{fs}	[m/s]	*Freestream velocity at* δ_{100}
d	[mm]	*Plate Thickness*
h	[mm]	*Free shear layer thickness*
f	[Hz]	*Frequency*
k	[1/m]	*Wave number*
c	[m/s]	*Wave speed*
x		*Cartesian co-ordinates in streamwise direction*
y		*Cartesian co-ordinates in vertical direction*
z		*Cartesian co-ordinates in spanwise direction*
CFD		*Computational Fluid Dynamics*
LES		*Large-eddy simulation*
LPT		*Low-pressure turbine*
K-H		*Kelvin-Helmholtz*
T-S		*Tollmien–Schlichting*
APG		*Adverse pressure gradient*

COMPUTATIONAL DETAILS

A separated boundary layer transition under an imposed pressure distribution on a flat plate of thickness (d = 12.8 mm) with an elliptic leading edge is studied. A specific contour surface is employed on each side of the flat plate as shown in Figure 1 to mimic the pressure distribution of T106 high-lift turbine blade. The geometry and flow conditions in the current

study are selected to match as closely as possible to those used in an experimental study by Coull *et al*. [4] so that the current LES results can be validated against the experimental data, which were also used for validation in a previous LES study by Nagabhushana *et al*. [8]. The current computational domain has a total length of 1315 mm in the streamwise direction and virtually all important flow features occur in a region starting from the leading edge as shown in a rectangular box named as "Test Section" in Figure 1 with a length of 500 mm, denoted as *So*. The co-ordinate system origin is at the leading edge point (stagnation point) and the inlet boundary is located upstream at -465 mm. The spanwsie size of the computational domain is 100 mm which is more than sufficient for the recommended spanwise size according to previous studies [5, 6]. The inlet height is 644 mm and the outlet height is 377 mm. A uniform velocity, U_{in} = 1.34 m/s, has been applied at the inlet to achieve the mean free stream velocity, U_{out} = 2.5 m/s, at the end of the test section (x/So = 1) according to the experiment. The resultant Reynolds number in terms of *So* and U_{out} is *Re* = 84000.

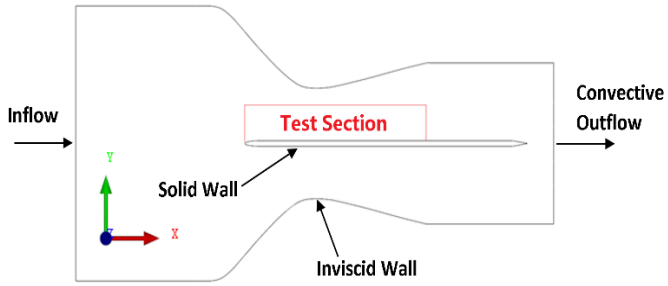

Figure 1 Schematic of computational domain

A numerical tripping method was employed to generate the desirable free stream turbulence intensity [6, 7]. The tripping plate is located upstream of the leading edge at x/*So* = -0.92. After initial damping of uncorrelated high frequency contents realistic turbulence is sustained, resulting in approximately 2.9% turbulence intensity near the leading edge, very close to the experimental value of 3%.

A finite volume in-house LES code, based on multi-block curvilinear structured grid with co-located mesh arrangement, is used. When solving the momentum equation, the diffusive term is discretised by the central difference scheme. Rhie-Chow pressure smoothing is added to the convection term to suppress pressure-velocity decoupling. The temporal discretisation is done by a single stage backwords Euler scheme. The SIMPLE algorithm is used to relate the discrete continuity equation face velocities to the discrete pressure field in the momentum equation. More details of the CFD code can be found in [7].

As shown in Figure 2A, about 5 million mesh points in total are employed in the inner and outer regions, with mesh points in x, y, z directions as: (n_x,n_y,n_z)=(428,130,50) in the outer region. C-grid is used for refinement in the inner region around the flat plate surface. Detailed view of the mesh around the flat plate leading edge is shown in Figure 2B. Based on the friction velocity further downstream at x/*So* = 1.5, y^+ of the nearest cell to the wall is about 1, the streamwise mesh resolution inside the test section, Δx^+, is about 15 and the spanwise mesh resolution $\Delta z^+ \approx 20$. The time step size of 1.0^{-4} second is used to ensure that the maximum CFL number is below 0.3.

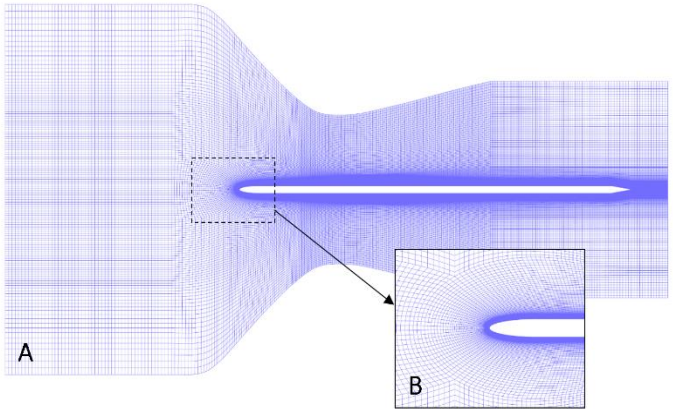

Figure 2 A: overall view of the mesh, B: detailed view of the mesh around plate leading edge

The initial simulation ran for 5 flow-through times to allow for full establishment of flow field. Mean data were gathered over further 5 flow-through times with samples taken every time step, and time series data were also collected at every time step for obtaining spectra and so on.

MEAN FLOW FIELD

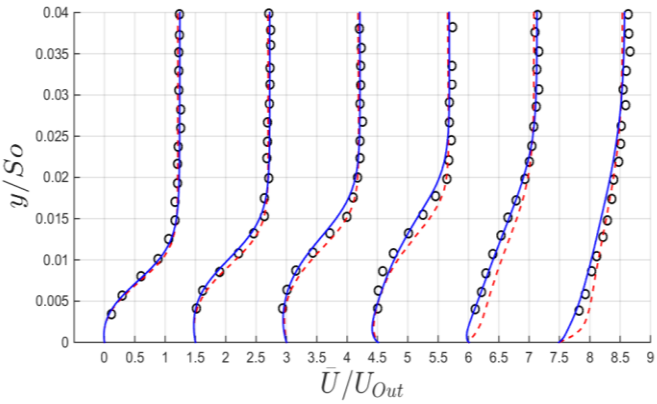

Figure 3 Mean velocity profiles, *x/So*=0.65, 0.70, 0.75, 0.80, 0.85, 0.90, Present LES (solid line), Exp. data (symbols), Previous LES (dashed line)

Figure 3 shows the mean streamwise velocity profiles along y-direction at six streamwise locations. Results from the current simulation compare well with the experimental data, having a closer agreement with the experimental data than the previous LES results [8] obtained from a 6th order central difference LES code using variational multi-scale approach (VMS) [9]. In such

approach, components are divided into large and small scale and Naiver Stoke equation is solved for each scale. The unresolved sub-grid scale stress term in the large-scale equation is assumed to be zero, and it is modelled by the conventional eddy-viscosity model in the small-scale equation. The VMS is employed to overcome the weakness of the Smagorinsky model whereas this problem is addressed in the current study by using a dynamic approach with the Smagorinsky coefficient evaluated locally. In addition the mesh resolution is also very good so that the current results agree slightly better with the experimental data than the previous LES results.

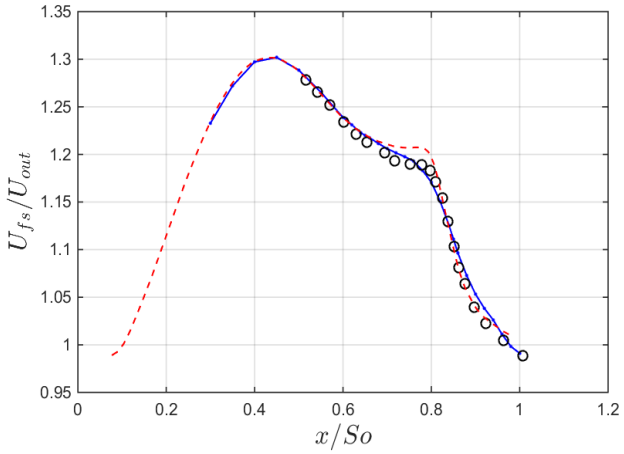

Figure 4 Streamwise velocity distribution, Present LES (solid line), Exp. data (symbols), Previous LES (dashed line)

Figure 4 presents comparison between the current predicted streamwise velocity distribution along x-direction in the free stream region and the experimental data, and the previous LES results. It can be seen clearly from this figure that a good agreement has been obtained between the current LES results and the experimental data, especially in the region just before *x/So* = 0.8 the current LES is much closer to the experimental data than the previous LES results.

Due to the change in local pressure distribution along the streamwise direction, from favourable to adverse pressure gradients, the boundary layer separates at about *x/So* = 0.6. The wall shear stress reaches zero at the separation and reattachment locations. Hence the mean separation bubble length can be obtained by locating the zero values of the mean wall shear stress. In the present study, the predicted mean separation and reattachment locations are at *x/So* = 0.61 and *x/So* = 0.87 respectively. The mean separation and reattachment points in the experimental study by Coull *et al.* [4] based on hot-film results and oil-and-dye flow visualisation, are at *x/So* = 0.54 and *x/So* = 0.85, and the prediciton from numerical study by Nagabhushana *et al.* [8] are at *x/So* = 0.62 and *x/So* = 0.86, respectively. The current and previous LES results agree very well with each other but the mean separation point is predicted a bit further dowbstream in both LES studies compared against the experimental data.

INSTANTANEOUS FLOW FEATURES

Streak structures have been found near the wall as shown in Figure 5 and some of them are formed well before the mean separation point. Those structures are named as Klebanoff streaks and have been well known to exist in attached boundary layer transitions. It is also understood that the formation of Klebanoff streaks originate from the free stream turbulence packets breakdown at the flat plate leading edge. The interaction of those free stream turbulence packets with the boundary layer leads to the formation of forward jet (local instantaneous streamwise velocity higher than the local mean velocity as shown in Figure 5) and backward jet within the boundary layer. Hence streak structures are actually those forward and backward jets.

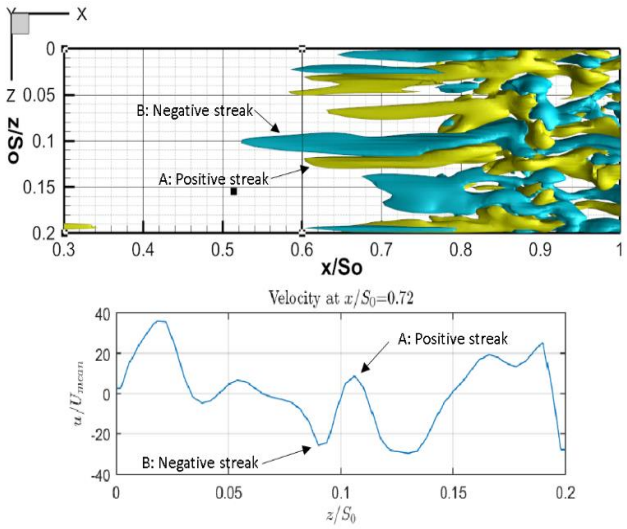

Figure 5 Top: wall-normal vorticity iso-surface; Bottom: streamwise-velocity from *x/So*=0.72 and *y/So*=0.016 along z/So.

The existence of Klebanoff streaks before the mean separation point indicates that the approaching boundary layer has been disturbed and possibly the well-known Tollmien-Schlichting (T-S) wave may have already occurred in the upstream attached boundary layer, hence leading to the formation of those streaks. Those streaks will have an impact on the separation and interact with the well established K-H rolls identified in previous separated boundary layer transition studies [5, 6, 10, 11]. The interactions can be observed in Figure 6 which presents four snapshots of instantaneous spanwise vorticity contours. At T = 0.02 second, streak A formed previously upstream bumps on top of the free shear layer while streak B is still further upstream. Lines are drawn to show their location in different times. Before streak A reaches the free shear layer region at about *x/So*=0.87 at T = 0.02 second, a K-H roll is clear observable there but when streak A arrives at this region at T = 0.04 second, no K-H rolls are visible there anymore. This is consistent with the findings by McAuliffe *et al.* [12] and they

suggested that both the viscous T-S instability and the inviscid K-H instability are at work in the transition process, and those two different modes of instability may interact with each other during the transition process too. When streaks pass over the free shear layer region, the K-H mode is enhanced leading to serve distortion of coherent K-H rolls or even break up of those rolls so that they are not visible. During the gap between two streaks the K-H instability is the dominant mode in the transition process. This may not be the case if the gap is too short for the K-H mode to be re-established, hence no K-H rolls are clearly observable at T = 0.06 and T = 0.08 seconds.

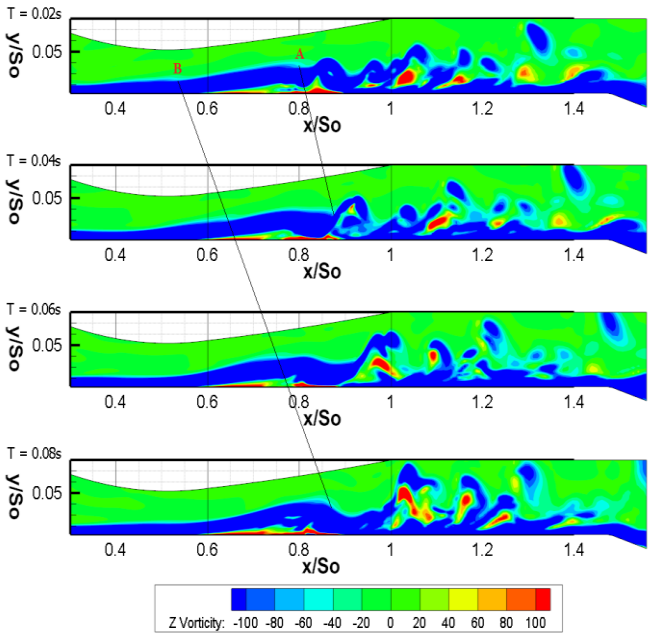

Figure 6 Instantaneous spanwise vorticity at z/So=0.2

THREE-DIMENSIONAL FLOW STRUCTURES

It has been demonstrated in previous studies that when the free stream turbulence level is low 2D K-H rolls are clearly visible in the early stage of separated boundary layer transition [5, 6, 10, 11]. However, in the current study those 2D K-H rolls are distorted severely due to elevated free stream disturbances and due to the oncoming streaks from upstream as shown in 6, leading to the formation of 3D structures rapidly. Under low free stream turbulence level downstream of the 2D K-H rolls certain 3D structures have been identified such as Λ-vortex which can also be observed occasionally in the current study as shown in Figure 8A. In addition, other kind of 3D structures, which may be formed due to the interaction between the streaks and the K-H rolls, are also visible as shown in Figure 8B. Mostafa and Yang [6] has demonstrated that the K-H instability is bypassed at a higher free stream turbulence level of 5.6% and further analysis is going to be presented in the next section to clarify if the K-H is by passed or not in the current study under the free stream turbulence level of 2.9%.

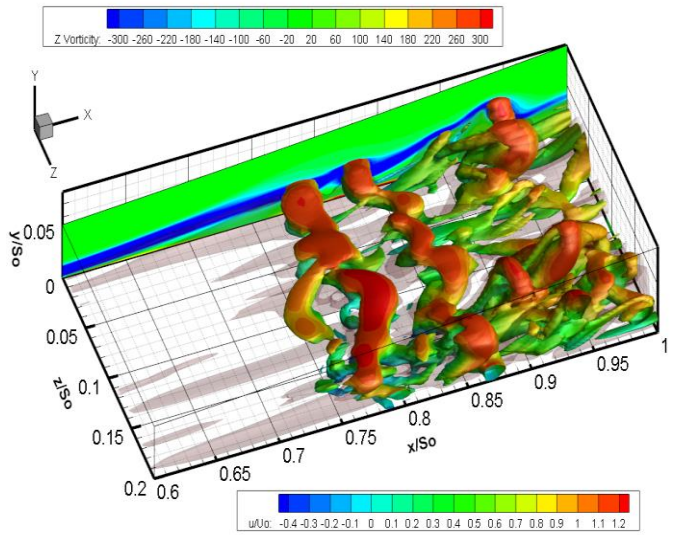

Figure 7 Q iso-surfaces of spanwise vorticity and streaks shown in grey

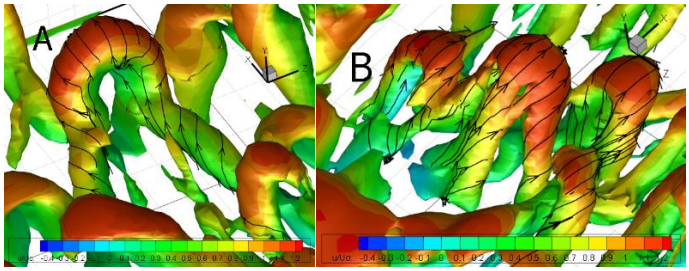

Figure 8 Two different types of 3D vortical structures

STABILITY ANALYSIS

To identify rigorously the existence of the K-H instability in the present study the approach taken by Yang *et al.* [5] is adopted here. The approach is based on the criterion given by S. Chandrasekhar [13]: for two layers of uniform flow of constant density with different velocities, the free shear layer formed in such a case with hyperbolic tangent velocity profile is unstable via the Kelvin-Helmholtz instability if $0<kh<1.0$, where k is the wave number and h is the free shear layer thickness.

The occurrence of initial unsteadiness in the current study is at about x/So = 0.75 as indicated in Figure 9 which presents instantaneous velocity components. The shear layer thickness at this location is h=0.018So. Hence the unstable wave number region for the K-H instability to occur is $0<k<1.0/h$, i.e, $0<k<55.56/So$. k can be found from characteristic frequency f, $k=2\pi f/c$, where c is the wave speed at the inflection point where the second derivative $d^2U/dy^2 = 0$. In the current study the wave

speed is $c = 0.8U_{out}$. Hence the unstable region of characteristic frequency for K-H instability is $0<f<7.07U_{out}/So$.

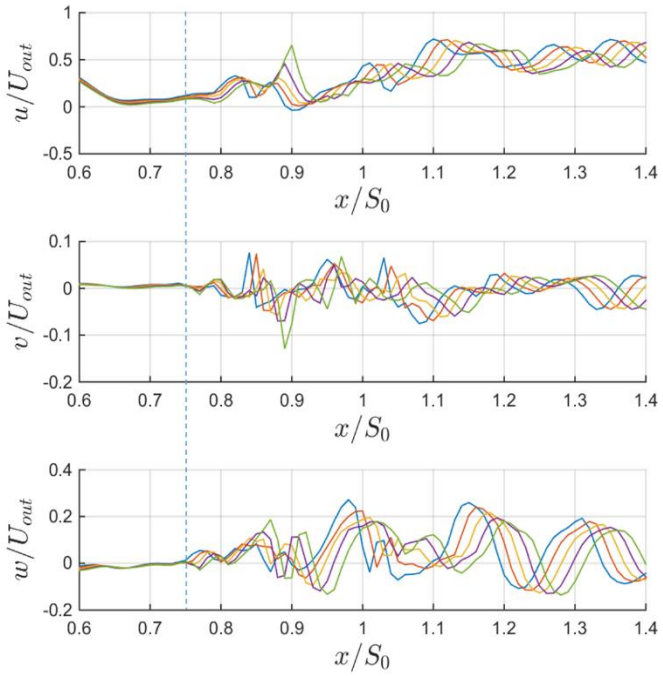

Figure 9 Instantaneous streamwise, wall-normal and spanwise velocity components at five arbitrary times along the streamwise flow direction

Power spectrum density (PSD) is used to find the characteristic frequency as shown in Figure 10 and a mild characteristic frequency peak is observed at $f = 2.8U_{out}/So$. This value is well within the unstable region of the K-H instability frequency ($0< f < 7.07U_{out}/So$). Upon repeating this analysis to the upstream and downstream locations at x/So=0.742, and x/So = 0.784, the free shear layers at these locations also satisfy the unstable criteria of the K-H instability.

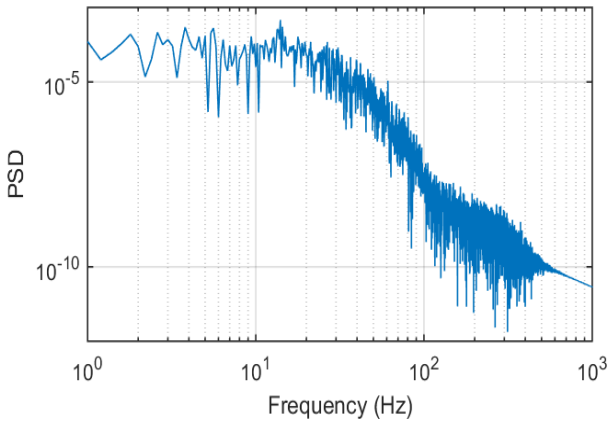

Figure 10 Power spectrum density of streamwise velocity fluctuation u' at $x/So=0.75$, $y/So=0.04$.

In a numerical study by Mcauliffe and Yaras [1], the maximum amplification frequency of the T-S wave is clearly observable in the spectrum of the free shear layer at the location near separation region. Their study was carried out under low freestream turbulence intensity of 1%, as well as condition of adverse pressure gradient. Whereas under 3% of freestream turbulence intensity in the current study, the same phenomenon is not observed, which indicates that in the current study the T-S wave is bypassed at a higher free stream turbulence level of about 3%. This is consistent with the established fact that the T-S wave would be bypassed if the free stream turbulence level is above 1%.

CONCLUSION

LES with a dynamic sub-grid scale model has been employed to study the separated boundary layer transition on a flat plate with an elliptical leading edge. A streamwise pressure distribution is imposed and the free stream turbulence intensity is about 3% to simulate the LPT blade suction surface. The current predicted LES results agree well with the experimental data and the previous LES results.

The whole transition process has been visualized and. Klebanoff streaks have been observed upstream the mean separation location. It observed that the Klebanoff streaks interact with a full-span K-H roll, leading to the distortion of the K-H roll, and portion of the two-dimensional roll merges with the Klebanoff streaks and develop into chaotic three-dimensional structures rapidly downstream. Whereas the remaining undisrupted two-dimensional K-H rolls develop into Λ-vortex, indicating that the K-H instability is the main primary instability at work. This has been confirmed by quantitative stability analysis too but there is no evidence for the existence of the T-S wave in the attached boundary layer before the mean separation location. Nevertheless the Klebanoff streaks observed before the separation indicate that the T-S wave has been bypassed and transition process in this kind of situation may have started in the attached boundary layer before separation and a more rapid transition turbulence occurs after the separation due the interactions between the Klebanoff streaks and the K-H rolls.

REFERENCES

[1] S. K. Roberts and M. I. Yaras, "Large-Eddy simulaiton of transition in a separation bubble," *ASME*, vol. 128, pp. 323-328, 2006.

[2] B. R. McAuliffe and M. I. Yaras, "Numerical study of instability mechanisms leading to transition in separation bubble," *ASME*, vol. 130, pp. 1-8, 2008.

[3] J. D. Hughes and G. J. Walker, "Natural transition phenomena on an axial compressor blade," *ASME*, vol. 123, pp. 392-401, 2001.

[4] J. D. Coull and H. P. Hodson, "Unsteady boundary-layer transition in low-pressure turbines," *J. Fluid Mech*, vol. 681, pp. 370-410, 2011.

[5] Z. Yang and P. R. Voke, "Large-eddy simulation of boundary-laryer separation and transition at a change of surface curvature," *J. Fluid Mech*, vol. 439, pp. 305-333, 2001.

[6] M. Langari and Z. Yang, "Numerical study of the primary instability in a separated boundary layer transition under elevated free-stream turbulence," *Physics of Fluids*, vol. 25, pp. 1-12 2013.

[7] C. D. Pokora, W. A. McMullan, G. J. Page, and J. J. McGuirk, "Influence of a numerical boundary layer trip on spatio-temporal correlations within LES of a subsonic jet," presented at the 17th AIAA/CEAS Aeroacoustics Conference, Portland,Oregon, 2011.

[8] V. Nagabhushana, P. G. Tucker, R. J. Jefferson-Loveday, and J. D. Coull, "Large eddy simulation in low-pressure turbines: Effect of wake at elevated free-stream turbulence," *International Journal of Heat and Fluid Flow*, vol. 43, pp. 85-95, 2013.

[9] T. J. R. Hughes, L. Mazzei, and K. E. Jansen, "Large eddy simulation and the variational multiscale method," *Comput Visual*, vol. 3, pp. 47-59, 2000.

[10] Z. Yang and I. E. Abdalla, "Effects of free-stream turbulence on large-scale coherent structure of a separated boundary layer transition," *International Journal for Numerical Methods in Fluids*, vol. 49, pp. 331-348, 2005.

[11] I. E. Abdalla and Z. Yang, "Numerical study of the instability mechanism in transitional separating-reattaching flow," *Internatioanl Journal of Heat and Fluid Flow*, vol. 25, pp. 593-605, 2004.

[12] B. R. McAuliffe and M. I. Yaras, "Transition mechanisms in separation bubbles under low- and elevated-freestream turbulence," *Journal of Turbomachinery*, vol. 132, pp. 1-10, 2010.

[13] S. Chandrasekhar, *Hydrodynamic and hydromagnetic stability*, 1968.